ASSOCIATIVE AND DISSOCIATIVE IONIZATION OF GASES ON IMPACT OF METASTABLE ATOMS

By
JOHN AUSTIN HERCE

A DISSERTATION PRESENTED TO THE GRADUATE COUNCIL OF
THE UNIVERSITY OF FLORIDA
IN PARTIAL FULFILLMENT OF THE REQUIREMENTS FOR THE
DEGREE OF DOCTOR OF PHILOSOPHY

UNIVERSITY OF FLORIDA
December, 1967

To

Sam and Archie

ACKNOWLEDGMENT

The author wishes to express his sincere appreciation to Professor E. E. Muschlitz, Chairman of his Supervisory Committee, for his assistance and guidance, to Dr. R. J. Cross, who was responsible for the design and construction of the molecular beam source, to Dr. K. D. Foster, for his helpful suggestions and aid in performing the experiments, and to the other members of his Supervisory Committee for their helpful suggestions in the writing of this dissertation.

The author is also grateful to the American Chemical Society Petroleum Research Fund for the financial assistance that made this work possible.

TABLE OF CONTENTS

LIST OF TABLES

LIST OF FIGURES

CHAPTER I

INTRODUCTION

In the past much of our knowledge of intermolecular forces has been obtained by relating certain macroscopic properties to the microscopic forces responsible for them. The theory of gaseous transport processes - such as diffusion, heat conductivity and viscosity - was developed on the basic assumption that the molecules behave like point-centers of force. In general, these calculations depended upon detailed information concerning the variation of the molecular velocity distribution of the gases, and unless the gases were in thermal equilibrium, these variations could not be calculated directly. Frequently, very complicated theories are required to circumvent a lack of detailed knowledge of the interactions taking place. With the advent of molecular beam techniques, however, direct and often detailed information may be obtained regarding the intermolecular forces acting between atoms and molecules.[1,2]

A molecular beam may be defined as a unidirectional beam of neutral atoms or molecules at such low pressures that the effect of molecular collisions is essentially negligible. Ordinarily a molecular beam is formed by effusive flow of atoms or molecules through an orifice, with subsequent beam definition by one or more apertures aligned with the first. The earliest molecular beam experiments were those of Dunoyer in 1911.[3] His apparatus consisted of an evacuated

glass tube divided into three separately evacuated chambers. Sodium metal introduced into the first chamber was vaporized, whereupon a deposit of sodium was noted in the third chamber. He concluded from these experiments that the sodium atoms traveled in straight lines. The work of Stern and Knauer in 1926[4,5] provided the basis for many of the molecular beam techniques which have followed. One of the most important applications of molecular beams has been the measurement of spins and magnetic moments of both atoms and molecules by deflection in an inhomogeneous magnetic field.[6,7]

Collisions between particles may be classified as either elastic or inelastic processes. This classification is solely dependent on whether the particles undergoing collisions suffer a change in either mass or internal energy. Elastic collisions may be viewed in terms of the interaction potential existing between the colliding species; on the other hand, inelastic collisions involve a change in the internal energy of the reactants or an atom-interchange between them.

A chemical reaction implies an inelastic collision between the reacting species. Excess energy may appear either as a change in the internal energy or kinetic energy of translation of the interacting particles. Scattering experiments have furnished a means for investigating the kinematics of these reactions and enable the detection of short-lived reaction intermediates.[8] It is obvious that these short-lived species could never be studied by a measurement of some bulk property.

Collisions of excited neutrals with thermal energy atoms

or molecules resulting in ionization were discovered by Penning in his studies of gaseous discharge processes.[9] On introducing an argon impurity into a pure helium discharge, a larger current was attained than that measured for the pure helium discharge. Penning reasoned that this current enhancement resulted from the ionization of argon by metastable helium atoms. Hornbeck and Molnar[10] investigated the formation of rare gas molecular ions and concluded that these ions result from collisions between excited and ground state rare gas atoms. Sholette and Muschlitz[11] obtained the first cross sections for ionizing collisions of metastable helium atoms in various gases. Čermák and Herman[12] made the first comprehensive study of the ionization and fragmentation of the lower hydrocarbons by metastable rare gas atoms.

It is the purpose of this work to investigate associative and dissociative ionization resulting from impact of thermal energy helium and neon metastable atoms on various gases.

CHAPTER II

SURVEY OF METASTABLE ATOMS AND INELASTIC PROCESSES

Excited atoms or molecules with lifetimes greater than a microsecond are generally described as metastable, the transition to the ground state being forbidden by the selection rules governing electric dipole radiation. These selection rules are:

(a) $\Delta J = 0, \pm 1 \quad J = 0 \not\leftrightarrow J = 0$

(b) $\Delta S = 0$

(c) $\Delta l = \pm 1$

where

l = orbital angular momentum of an electron

J = vector sum of L and S

L = orbital angular momentum = $\sum_i li$

S = spin angular momentum.

The 2^1S_0 and 2^3S_1 metastable states of helium lie 20.61 and 19.82 eV above the ground state, respectively. Decay of the 2^1S_0 states to the ground state is forbidden by selection rules (a) and (c), while (b) and (c) forbid transitions of the 2^3S_1 state to ground. Similarly, neon has two metastable states, $^3P_2$ and $^3P_0$, which lie 16.62 and 16.71 eV above the ground state.

Although forbidden by electric dipole processes, decay of metastable atoms to the ground state can occur by double photon

emission and magnetic dipole radiation. These latter mechanisms are about 10^{-5} as probable as ordinary electric dipole radiation, and, consequently, the lifetimes of these metastable states are on the order of a second. For comparison, lifetimes of excited states for which electric dipole radiation is allowed are approximately 10^{-9} second.

No experimental determination of the metastable helium lifetimes is available, but calculated lifetimes are on the order of one second or greater.[13] The 2^1S_0 metastable state can be quenched in the presence of a strong electric field. Holt and Krotkov[14] attained (90 ± 2) per cent quenching of the 2^1S_0 state of helium at a field strength of 226 kv./cm.

Beams of excited particles have been produced by gaseous discharge and electron impact. The former method usually results in a higher intensity of the excited species, but is not very selective and produces several atomic or molecular excited states. Selective excitation of a beam of neutrals can be attained by electron impact, but care must be taken to ensure that beam collimination is not destroyed by recoil of the excited particles. Normally, the beam of controlled energy electrons is located either directly in front or in back of the first colliminating aperture of the beam source.

Electron ejection from metal surfaces by incident metastable atoms is known to occur, and this property has often been used for metastable atom detection. Oliphant[15] first observed electron ejection from a gas-covered molybdenum surface by metastable

helium atoms. Greene[16] extended this work to include argon and neon metastable atoms. Stebbings[17] measured the electron yield from a gas-covered gold surface. He concluded that his value of 0.29 for the electron yield represented that for the triplet state of metastable helium. More recently, MacLennan[18] reported the absolute electron yield of helium and neon metastable atoms incident on an atomically clean polycrystalline tungsten surface. The value for helium is 0.306 $\pm$ 0.025, where the 2^1S_0 and 2^3S_1 yields are equal within his experimental error; the neon value is 0.215 $\pm$ 0.020. This latter determination did not include resolution of the contributions of the two metastable states.

Excitation of helium by electron impact has been studied by various methods. The most recent determinations of excitation efficiency curves of the singlet and triplet states of helium are those of Čermák[19] and Dugan, et al.[20] Čermák obtained separate excitation functions in the energy range 20-60 eV for 2^1S_0 and 2^3S_1 helium from studies of the kinetic energy of the electrons released in the Penning ionization of argon by metastable helium atoms. Dugan, et al. obtained these excitation functions in the range 25-135 eV by observing the deflection of the beam of metastable atoms in an inhomogeneous magnetic field. These authors report the ratio of the singlet to triplet functions which vary from 0.26 to 2.37 in the energy range studied.

Several types of ionizing collisions between a metastable atom and an atom or molecule are possible, e.g.:

$$X^* + Z \rightarrow X + Z^+ + e^- \qquad \text{(II-1)}$$

$$X^* + Z \rightarrow XZ^+ + e^- \qquad \text{(II-2)}$$

$$X^* + Y_2 \rightarrow X + Y_2^+ + e^- \qquad \text{(II-3)}$$

$$X^* + Y_2 \rightarrow X + Y^+ + Y + e^- \qquad \text{(II-4)}$$

$$X^* + Y_2 \rightarrow XY_2^+ + e^- \qquad \text{(II-5)}$$

$$X^* + Y_2 \rightarrow XY^+ + Y + e^- \qquad \text{(II-6)}$$

The first of these, Penning ionization, represents the conversion of electronic excitation energy to ionization and kinetic energy. This process occurs in gaseous discharge and in the radiation chemistry of gases.[9,21] Other cases of Penning ionization are (II-3) and (II-4), where the molecule-ion may be formed in an excited repulsive state resulting in dissociative ionization. It is possible in all cases that these ions may be formed in excited states, but usually the reaction is nearly resonant, for the electron can carry off the excess energy. Herman and Čermák[22] have studied reactions of types (II-1) and (II-2) and obtained the ratio of cross sections for the formation of Hg^+ and $ArHg^+$ for collision of metastable argon atoms with mercury atoms. Muschlitz and Weiss[23] cite ionization cross sections for the production of O_2^+ and O^+ in the $He^* - O_2$ system. Individual total ionization cross sections for the 2^1S_0 and 2^3S_1 metastable states of helium on various gases have been reported by Sholette and Muschlitz.[11]

Reaction (II-5) was first investigated by Hornbeck and Molnar.[10] For this process to be energetically possible at thermal energies, it is necessary that the ionization potential of X^* be less than the energy required for the process $XY_2^+ \rightarrow X^+ + Y_2$. These same authors

also investigated the formation of the homonuclear rare gas molecular ions (II-2) and concluded that they result from the reaction of an excited, not necessarily metastable, rare gas atom with its ground state counterpart. Kaul, et al.[24] have also investigated these same processes and have shown that there are at least two excited states of helium contributing to the formation of He_2^+. Kaul[25] has extended these studies to other rare gas systems and reported the lifetimes of those excited states responsible for the production of the rare gas homonuclear ions. Munson, et al.[26] have measured the appearance potentials for all homonuclear and heteronuclear rare gas ions with the exceptions of $HeXe^+$ and the radon compounds.

Since the beam of metastable helium atoms produced by electron impact is composed of atoms in more than one metastable state, the following treatment has been developed to isolate the contribution of each excited state to the total ionization. This has been applied to the systems in which the composition of the metastable beam is known (metastable helium) and more than one ion was produced in the collision.

Let

A_0 = per cent ion abundance produced by the mixed beam

A_1 = per cent ion abundance due to $(2^1S_0)He^*$

A_3 = per cent ion abundance due to $(2^3S_1)He^*$

$R = (2^1S_0)He^*/(2^3S_1)He^*$ = ratio of metastable states in the mixed beam.

If the observed ion abundance is considered as the sum of contributions

from each metastable state, then

$$A_0 = [R/(1 + R)]\, A_1 + \{1 - [R/(1 + R)]\}\, A_3$$
$$= (A_1 - A_3)[R/(1 + R)] + A_3, \qquad \text{(II-7)}$$

where $R/(1 + R)$ = fraction of (2^1S_0)He in the mixed beam.

The value of $R/(1 + R)$ has been calculated from the results of Dugan, et al.[20] who measured the ratio $(2^1S_0)\text{He}/(2^3S_1)\text{He}$ as a function of the energy of the electron beam used to produce these excited states. The above treatment suggests that a plot of the experimentally measured ion abundances expressed as a per cent of the total ionization versus $R/(1 + R)$ should result in a straight line of slope $(A_1 - A_3)$ and intercept A_3. These data may then be extrapolated to yield the per cent ionization due entirely to a single metastable species. From knowledge of the total ionization cross section for a particular system, that is a measure of the total ionization occurring irrespective of the identity of the product ions, individual ionization cross sections for each metastable species can be calculated.

CHAPTER III

DESCRIPTION OF APPARATUS

The experimental arrangement used for this work consists of a 12 inch radius-of-curvature, 60° sector, magnetic deflection, first order direction-focusing mass spectrometer modified for molecular beam experiments. A detailed drawing of the beam source, electron gun, collision chamber and ion accelerating-ion focusing lens is shown in Figure 1.

The atomic beam was produced by introducing the beam gas through an array of seven-micron-diameter glass capillaries affixed to the leading edge of the bellows. This arrangement provides an adjustable beam source having three degrees of freedom for the purpose of alignment. The source produces a 1/2 inch long by 0.030 inch wide beam. A portion of the atomic beam is excited in the source region by an electron beam traversing region N. The resultant beam composed of metastable atoms and ions then passes through a 1/2 inch long and 0.040 inch wide slit, D, which serves only to define the two separately pumped regions. The beam enters the collision chamber through a 1/2 inch long slot of adjustable width which was set at 0.030 inches.

Excitation of the beam gas was accomplished by electron bombardment. A cross-sectional view of the electron gun is given in Figure 1. This electron gun is of cylindrical symmetry and consisted

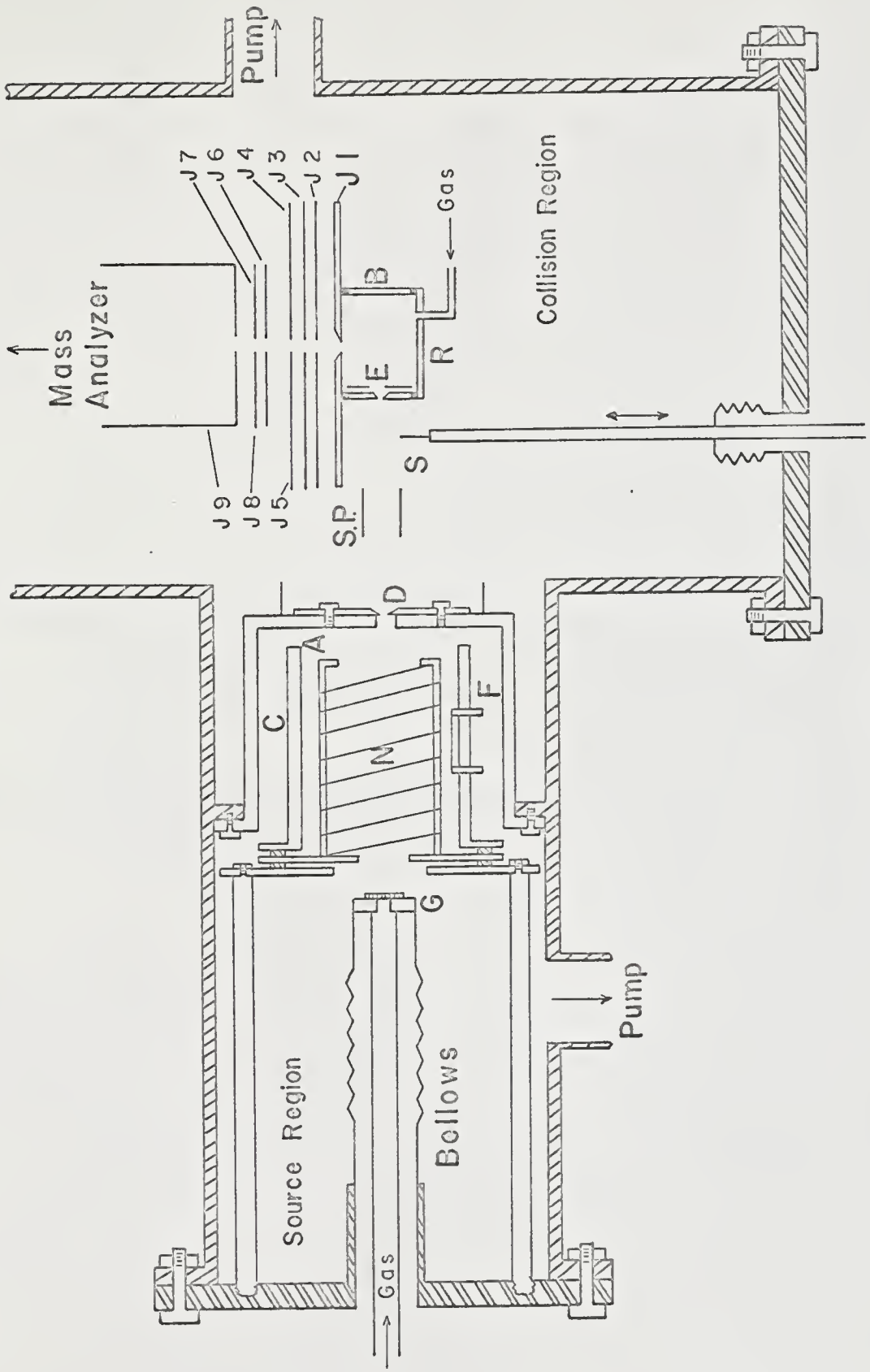

Figure 1. Cross Section of Apparatus.

of two concentric cylinders C and A with the filament F positioned in the annular region formed by them. Electrons were produced by thermionic emission from a directly heated iridium ribbon filament which had been thoriated by cataphoretic deposition as described by Muschlitz.[27] Electrons were accelerated and reflected across the equipotential region N by maintaining the outer cylinder C at a negative potential and the anode A at a positive potential with respect to the filament. The entire electron gun was fabricated from stainless steel. The anode consisted of 0.007 inch tungsten wire wound about six stainless steel rods. All spacers and insulators were ceramic. The entire electron gun assembly was insulated from ground and could be operated at a fixed potential with respect to ground by means of an auxiliary power supply.

A field of 8.3 kv./cm. was maintained across plates S.P. to deflect all ions and to quench any highly excited long-lived states present in the beam. A manually operated shutter S was placed directly behind these plates, so that the beam of metastables could be intercepted to obtain a zero reading.

The rectangular collision chamber was constructed from brass and heavily gold plated to obtain surfaces with equal electron-ejection efficiency. An additional isometric view of the collision chamber is given in Figure 2. Pressures in the collision region can be measured with the thermocouple gauge. The electrometer electrode E is employed for measurement of either total ionization cross sections or metastable beam intensity. Gaskets fabricated from teflon sheet provide electrical insulation and were found to be reasonably leak tight.

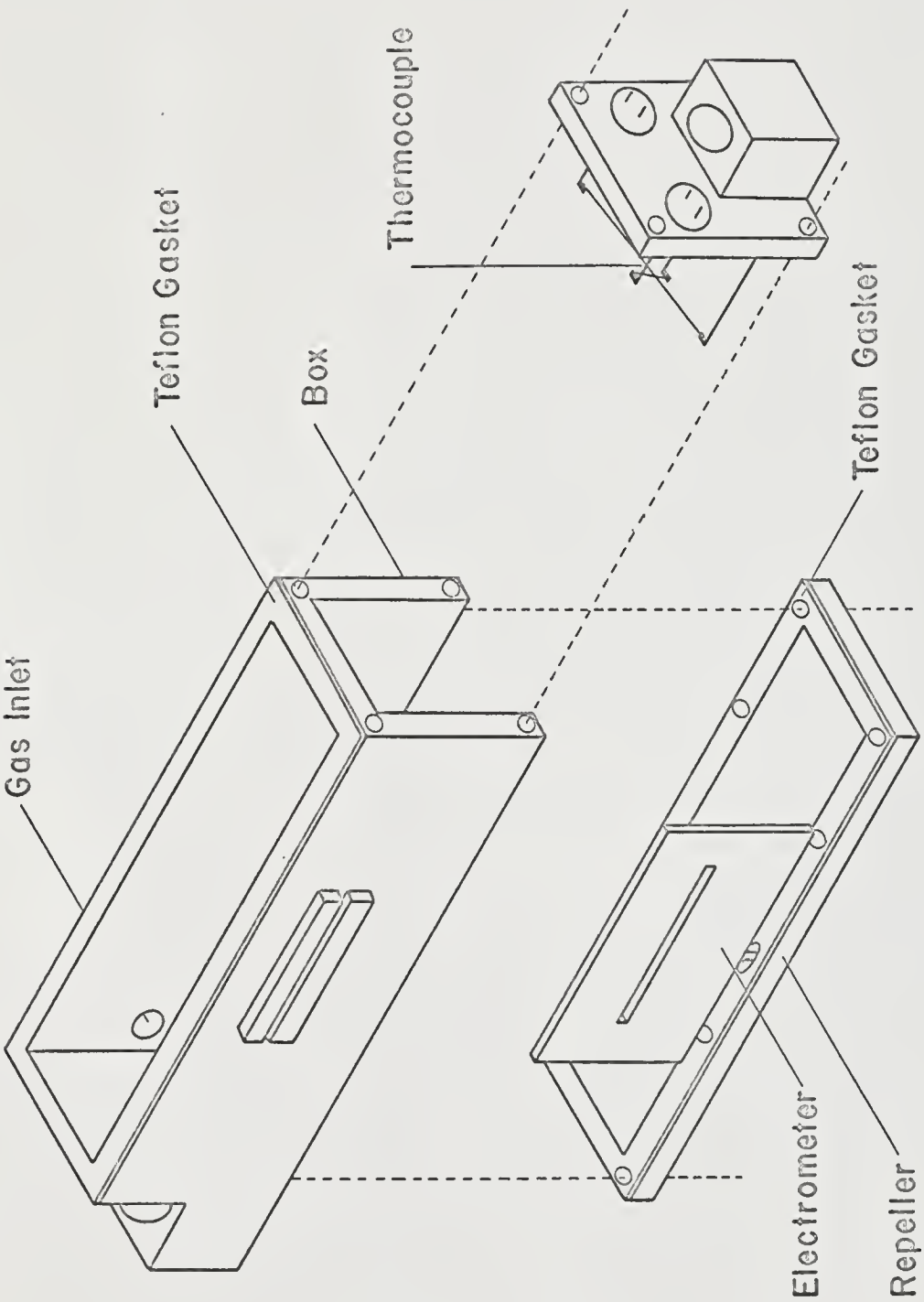

Figure 2. Isometric View of Collision Chamber.

In normal operation ions produced in the collision chamber are extracted at right angles to the incident metastable beam by a drawout field between the repeller R and J_1. Ions emerging from the slit in J_1 are gradually accelerated through a potential difference of five kilovolts provided by a Northeast Scientific Company, high voltage power supply. In the course of this acceleration the ion beam is focused by a series of electrostatic lenses, J_1 through J_9. The ion beam is then mass analyzed by a homogeneous magnetic field and finally impinges upon the first dynode of a secondary electron multiplier.

The field current of the analyzer is electronically regulated and swept by a power supply and control circuit constructed in this laboratory. The magnetic field is determined within 0.01 per cent by a Harvey Wells N.M.R. Gaussmeter. The electron multiplier is a twenty-stage device having copper-beryllium dynodes and manufactured by Nuclide Analysis Associates as their model EM-1. The multiplier has a measured gain of 9×10^5 for the mass 39 isotope of K^+ produced by surface ionization.

Ion intensity measurements were made by utilizing a pulse-counting method. The signal from the electron multiplier is amplified by a Tektronix, Inc., type 1121 amplifier followed by a linear pulse amplifier constructed in this laboratory. This pulse amplifier also performs as a pulse shaper and adjusts the baseline over-and under-shoot. A combination Beckman Counter, model 6020A and Beckman Printer, model 1453 provide both visual display and printed tape read-out of the ion intensity. Typical counting intervals of one to ten

seconds were employed.

An auxiliary vacuum system was used for gas manipulation and purification. The beam and scattering gases were introduced into their respective chambers through two Vactronic variable-leak valves. The helium, neon, argon and oxygen were obtained from cylinders and were purified by passage through an adsorption trap filled with degassed charcoal at low temperatures. These gases are estimated to have less than one part in 10^3 impurity as indicated by mass analysis. The methane used was Phillips Company reagent grade and guaranteed not to contain more than 40 parts impurity per 10^4. The methane-d_4, a Nichem Incorporated product, was observed to contain approximately one part impurity in 10^3 and was taken from a glass flask sealed directly into the auxiliary vacuum manifold. The krypton, an Air Reduction product, was obtained directly from cylinders and was guaranteed to contain no more than 36 ppm impurities.

CHAPTER IV

EXPERIMENTAL PROCEDURE

In order to produce and align the beam of metastable atoms, the following procedure was employed. Helium gas was leaked into the source region, and a pressure of 100 microns was maintained behind the capillary array (Figure 1). Excitation of the atomic beam was accomplished in region N by electron impact, and the resultant beam of metastable atoms was directed on the entrance slot of the collision chamber. A 90-volt potential difference across the deflecting plates S.P. was found to be sufficient to deflect any positive ions present in the beam. The entire collision chamber was maintained at -20 volts with respect to the electrode E, which was connected to a Cary, Model 31, vibrating-reed electrometer. An input resistance of 10^9 ohms was used. In this mode of operation, a negative current due to electrons ejected from the walls of the collision chamber by the metastable atoms was measured at E; this current is proportional to the metastable beam intensity, since

$$I_- = \gamma I_0, \tag{IV-1}$$

where:

I_- = measured electron current,

I_0 = metastable beam intensity, and

γ = metastable helium electron-ejection efficiency of gold.

By manual adjustment of the movable bellows arrangement, the signal I_- was maximized for optimum beam alignment.

The metastable beam current was then measured as a function of the energy of the electron beam (at constant electron beam current). The results are shown in Figure 3. It is seen that the metastable beam current exhibits a maximum at 30 electron volts and drops off at higher electron energies. Qualitatively, this agrees quite well with the appearance potential curve of He^* determined by Smith and Muschlitz.[28]

In the absence of a metastable beam but with a target gas in the collision chamber, electrons were purposely accelerated into the collision chamber by operating the electron gun at 100 volts negative with respect to ground and with zero deflection field across plates S.P. The mass spectrometer was then focused for optimum sensitivity on the parent ion resulting from electron impact. This procedure not only afforded a simple means of focusing the spectrometer but also provided a convenient means for calibration of the gaussmeter with an ion of known charge to mass ratio. This procedure was repeated for all scattering gases used in this study.

The scattering gas first used was argon with helium in the beam source. An ion peak appeared at mass 40, coinciding with the Ar^+ obtained by electron impact. To determine optimum extraction conditions for the Ar^+, the ion intensity was measured as a function of the voltage applied to the repeller R. Figure 4 shows a plot of ion intensity against this drawout potential. The ion intensity increased

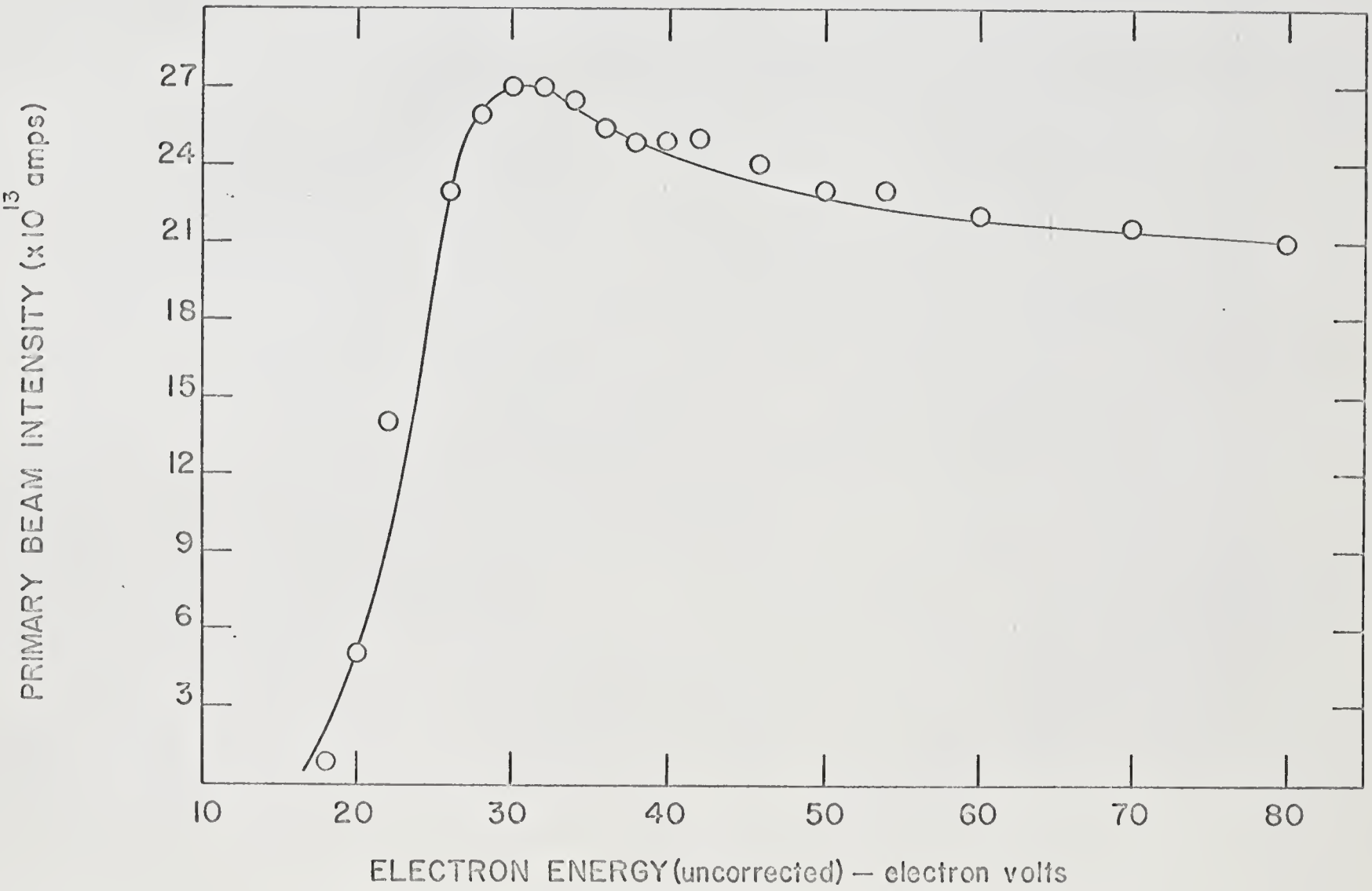

Figure 3. Primary Beam Intensity Versus Electron Energy.

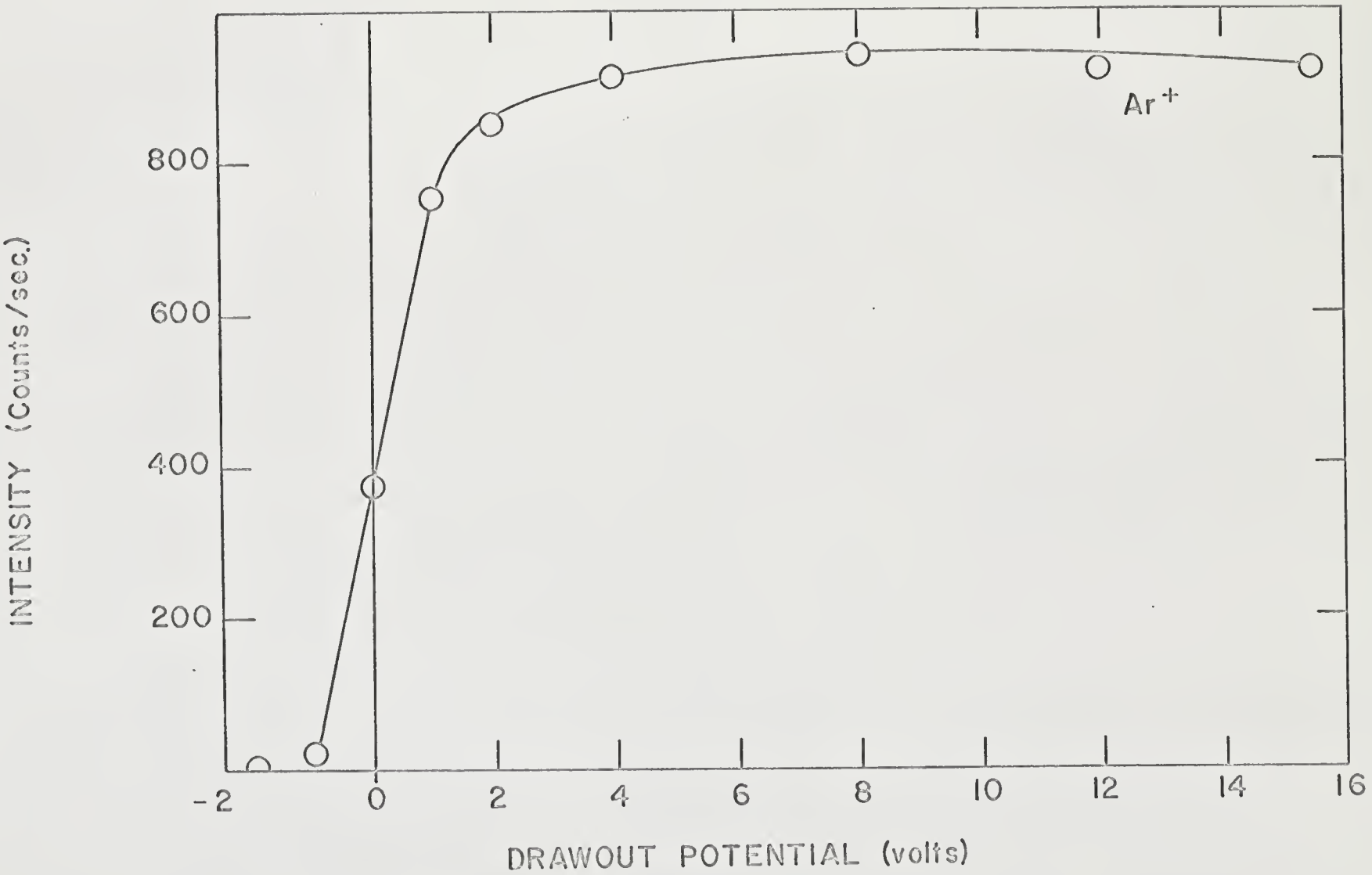

Figure 4. Ion Intensity Versus Drawout Potential.

quite rapidly at low drawout potential and saturated at +4 volts. Every scattering gas used in this study showed this same dependence, and all subsequent measurements were made at a 4 volt extraction potential.

A plot showing the pressure dependence of the Ar^+ and $HeAr^+$ ion intensities on argon backing pressure was made and is shown in Figure 5. A linear dependence of ion intensity with backing pressure was observed. Both ions vanished when the argon was pumped out of the collision chamber. Figure 6 shows a similar study for the Ne^* - Ar system. Using nitrogen as the scattering gas, only N_2^+ was observed. The N_2^+ intensity was measured as a function of the helium backing pressure. A linear dependence was found as shown in Figure 7. These observed linear dependences support the assumption that the ions were formed in a single collision process between the metastable atoms and the scattering gas. When the shutter S was positioned to intercept the beam of metastable atoms, no ions were observed. This served as additional proof of the nature and origin of the ion formation.

Excitation of the atom beam by electron impact, although reasonably selective, does not preclude the possibility that excited states other than the 2^1S_0 and 2^3S_1 metastable states were present in the beam. With this in mind, certain experiments were performed to substantiate the assumption that the beam of excited atoms contained only these metastable states. Table 1 summarizes these experiments. The first column lists the metastable atom involved in the collision process and the energy of its metastable states. Column

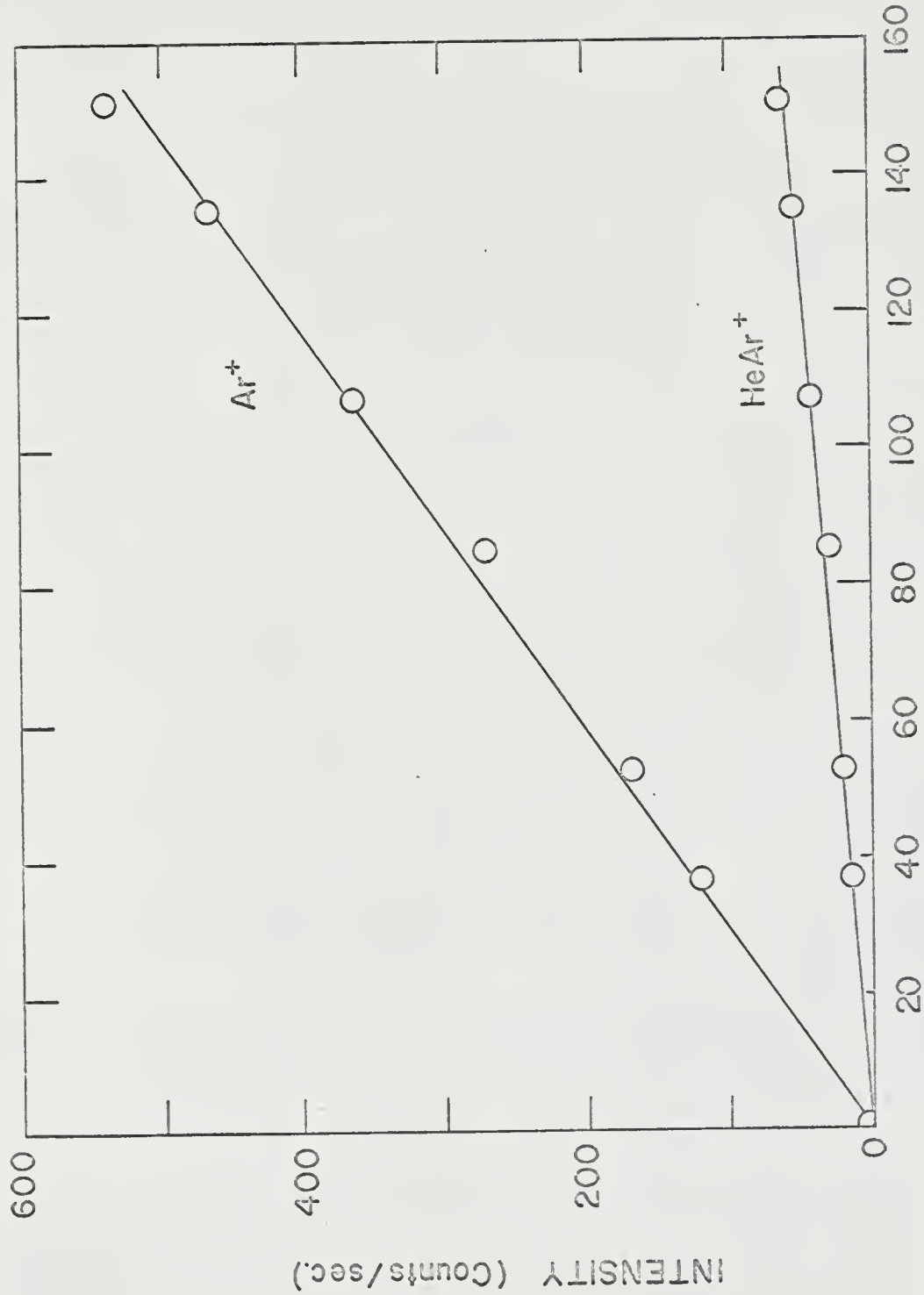

Figure 5. Ion Intensity Versus Argon Backing Pressure.

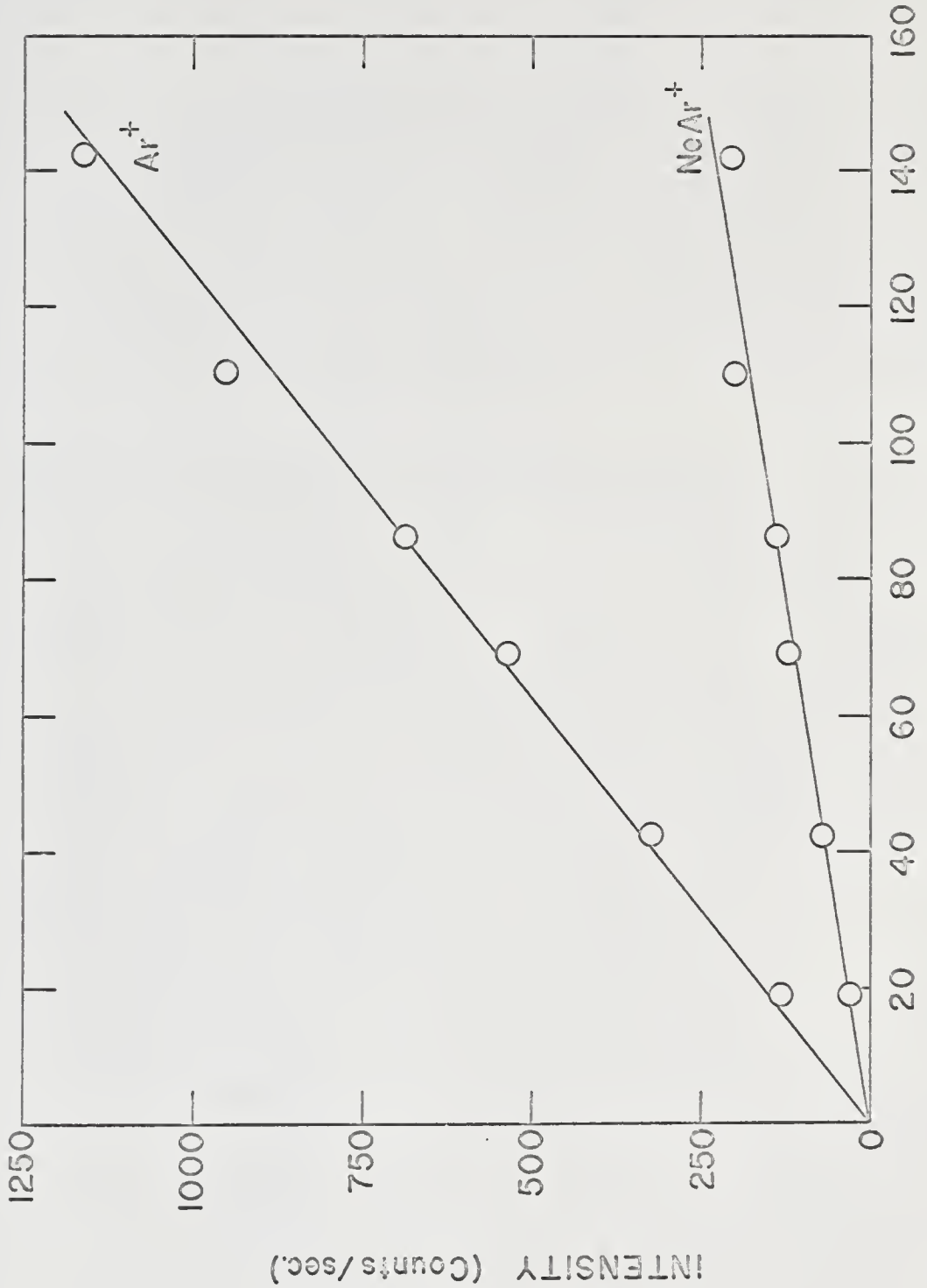

Figure 6. Ion Intensity Versus Argon Backing Pressure.

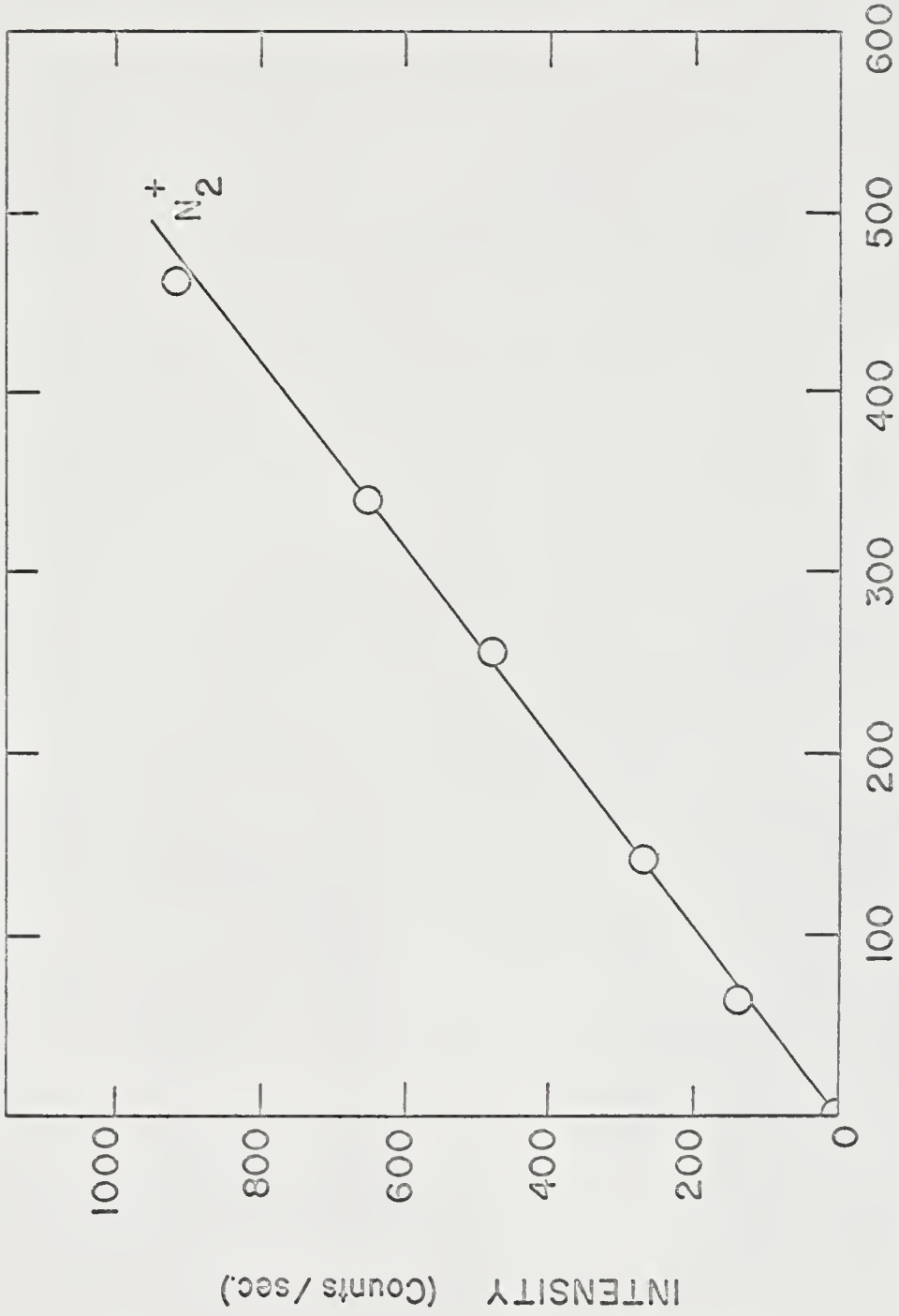

Figure 7. Ion Intensity Versus Helium Backing Pressure.

two lists the scattering gas. The positive ion or ions capable of being produced if highly excited states were present in the beam are listed in the third column. Appearance potentials for these ions and references are given in the last column. In all of the systems studied no ions were observed, indicating the absence of highly excited states. It has been recently observed that Ne^+ and He^+ ions are produced in collisions of highly excited neon and helium atoms in various gases.[29,30] The cross sections for such reactions are about four orders of magnitude larger than Penning ionization cross sections. No He^+ or Ne^+ ions were observed in this study.

The intensity of ions resulting from energetically allowed reactions was found to be independent of the quenching field maintained across S.P. (Figure 1) in the range 8.3 - 11 kv./cm. A simple calculation based upon the results of Holt and Krotkov[14] showed that 3 per cent of the 2^1S_0 metastable helium atoms were quenched in the 8.3 kv./cm. electric field used in all the experiments. This is a further indication that the beam of metastable atoms was free of highly excited states. The small change in the 2^1S_0 population due to the quenching field is not sufficient to affect the results within the experimental error of the measurements.

Of primary interest in this study was the variation in the amount and type of ionization process with respect to changes in the composition of the beam of metastable atoms. This was accomplished by measuring the ion intensities as a function of the energy of the electron beam. These ion intensities are listed in Appendix A as

Table 1. Determination of Absence of Highly Excited States in Beam.

Metastable Atom	Target Gas	Ion	Appearance Potential[a] (eV)
He^* (19.81 eV) (20.61 eV)	He	(He^+)	24.58
		(He_2^+)	23.3
	Ne	(Ne^+)	21.56
		($HeNe^+$)	23.4, 22.6
Ne^* (16.62 eV) (16.71 eV)	Ne	(Ne^+)	21.56
		(Ne_2^+)	20.9
Ar^* (11.55 eV) (11.72 eV)	He	(He^+)	24.58
		($HeAr^+$)	17.9

[a]See Ref. 26.

per cent ion abundances of the ions formed from collisions of metastable helium atoms on argon, krypton, oxygen, methane and methane-d_4. In the case of the He^* - Kr system, all isotopes of the parent ion were detected, but only the ion intensities involving the most abundant isotopes were used in the calculations. The Ne^* - Ar and Ne^* - Kr systems were also studied, and the experimental determinations are also given in the Appendix A.

Figures 8, 9, 10, 11 and 12 show the variation in the per cent ion abundances of the product ions with changing composition of the beam of metastable atoms. These plots have been constructed according to eq. (II-7). The fraction of singlet metastable helium atoms $R/(1 + R)$, which increases with increasing electron energy, was calculated from the results of Dugan, et al.[20] and is listed in Appendix B. Each experimental point represents an average value determined from three to four experimental measurements which agree within 3 per cent in all cases. Since the experimental data do fit a straight line, the assumption that the total amount of ionization may be treated as the sum of the individual contributions of each metastable state appears to be valid. This behavior also supports the initial premise that interactions between particles in the beam are negligible.

Since we are primarily concerned with the individual contributions of each metastable state, these values at $R/(1 + R) = 1$ and 0 and their most probable errors were determined by a least squares treatment.[31] For simplicity, the errors for each system will

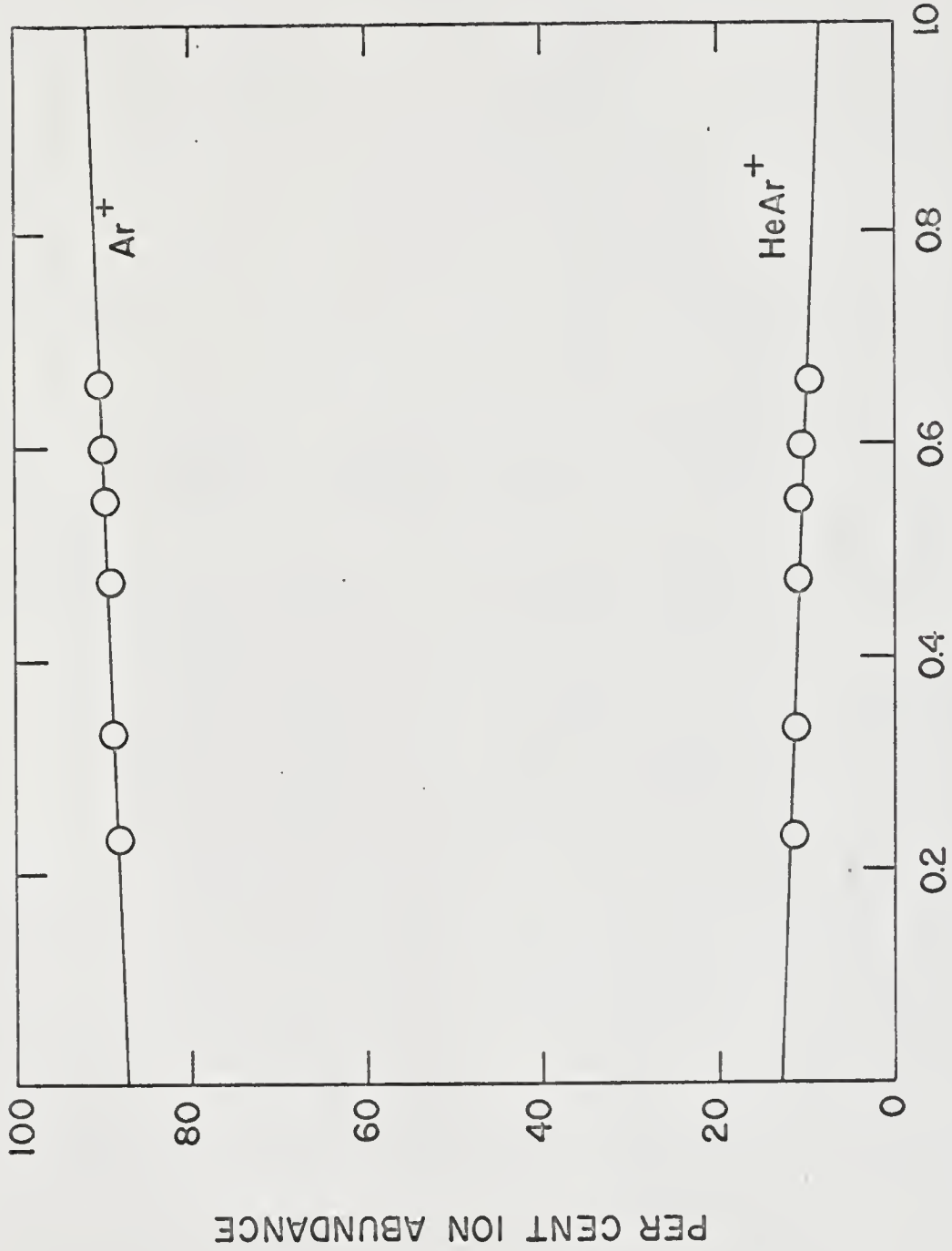

Figure 8. Per Cent Ion Abundance Versus R/(1 + R) for He^* + Ar.

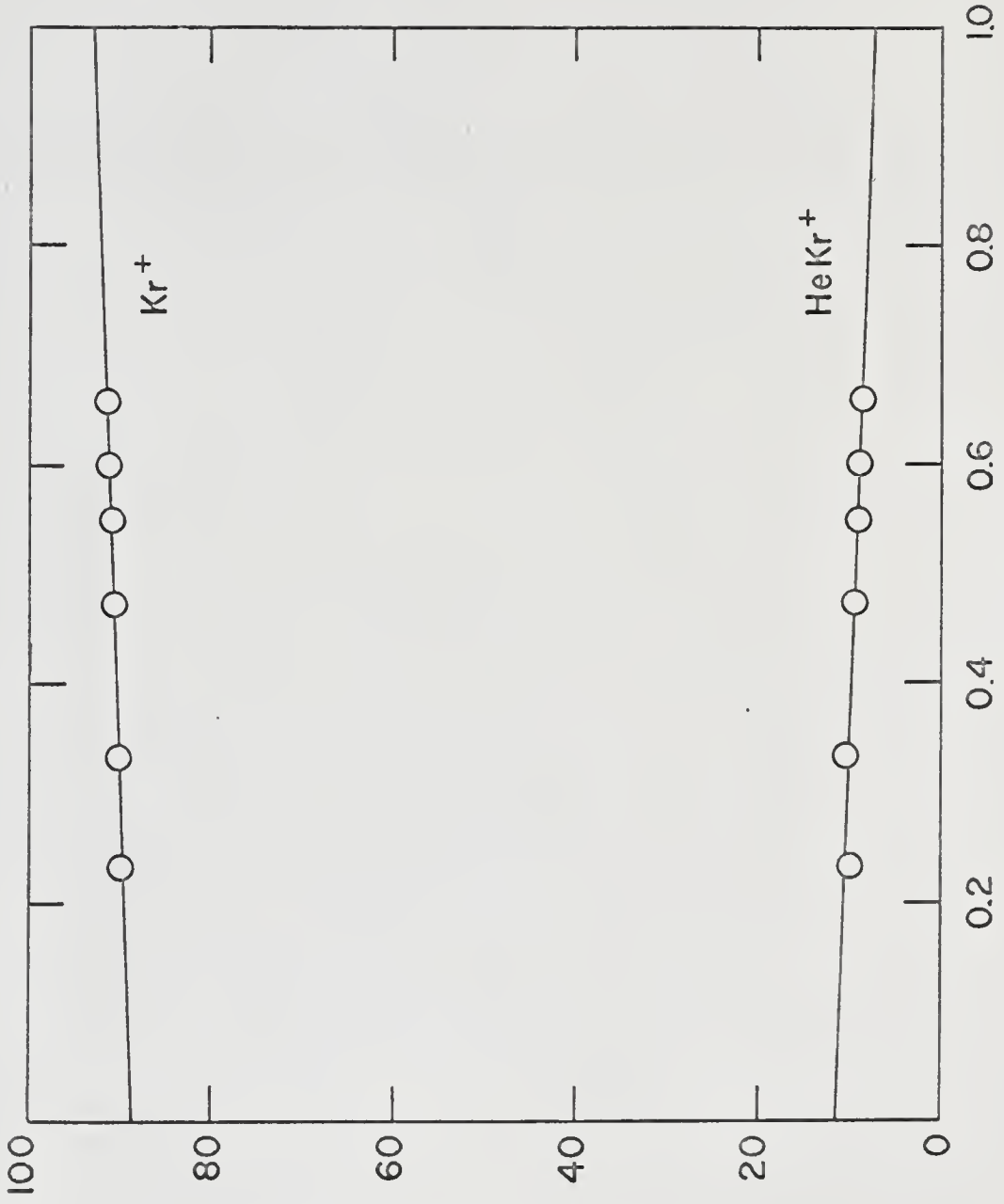

Figure 9. Per Cent Ion Abundance Versus R/(1 + R) for He^* + Kr.

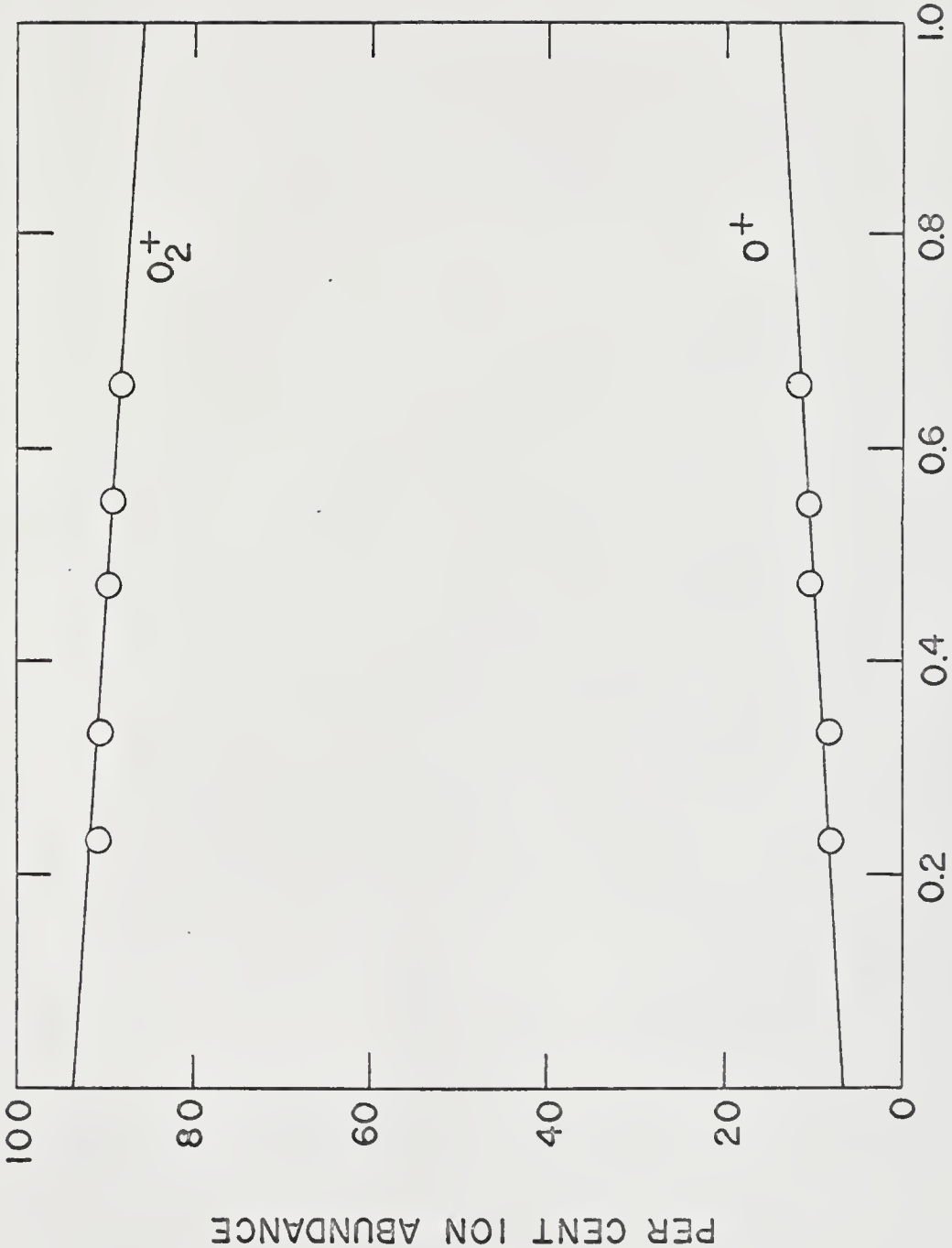

Figure 10. Per Cent Ion Abundance Versus R/(1 + R) for $He^* + O_2$.

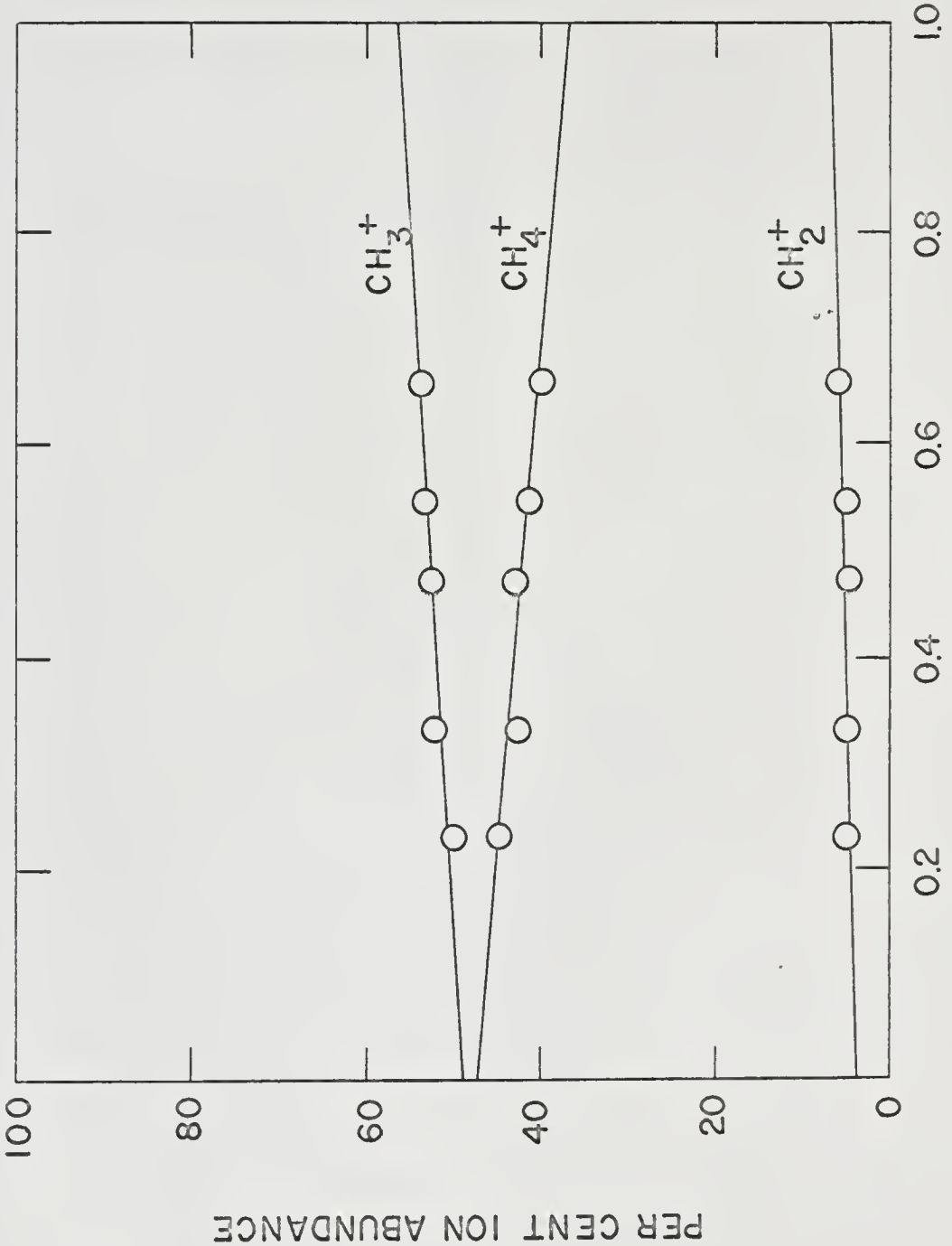

Figure 11. Per Cent Ion Abundance Versus R/(1 + R) for He^* + CH_4.

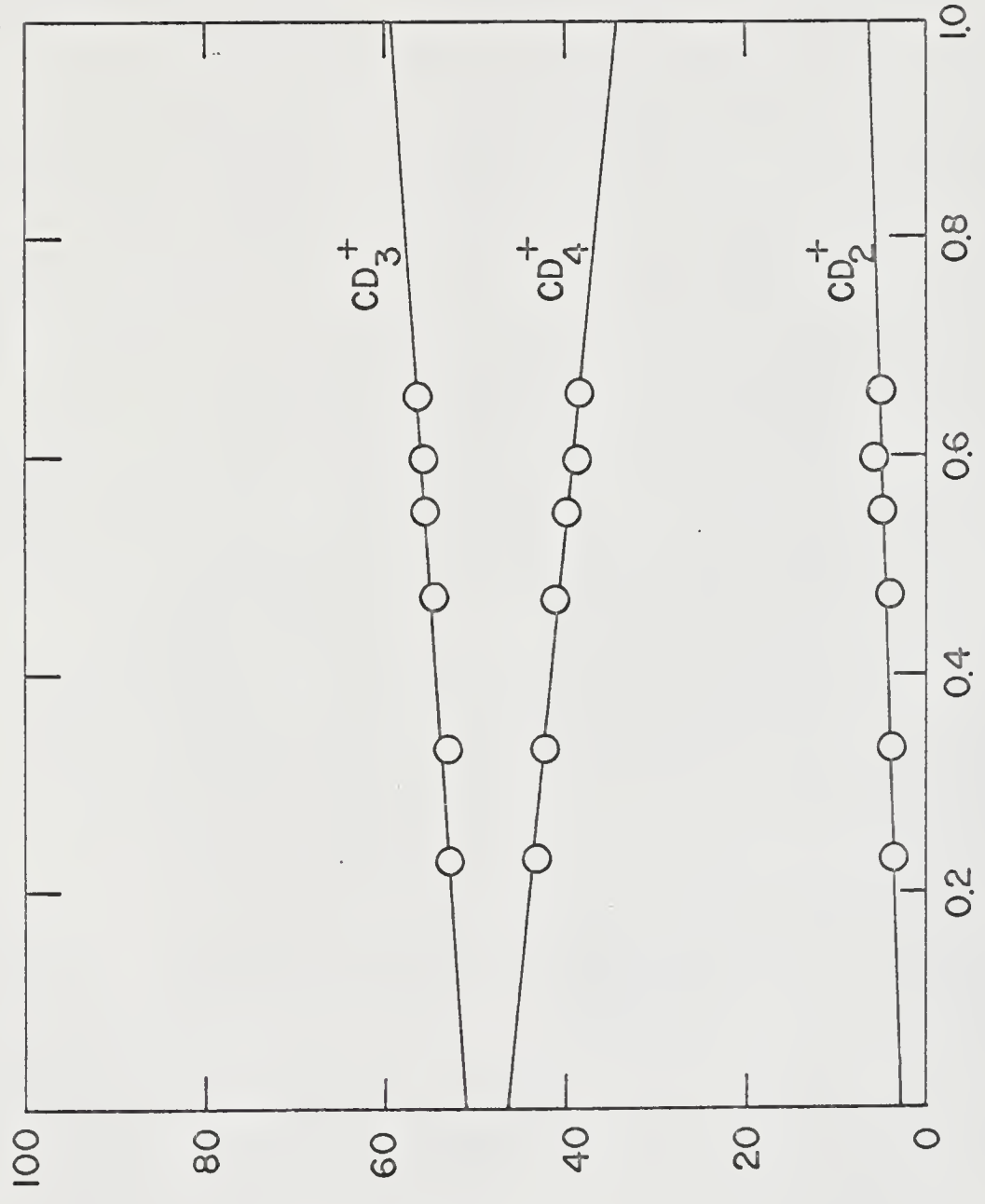

Figure 12. Per Cent Ion Abundance Versus R/(1 + R) for $He^* + CD_4$.

be tabulated in the discussion. Both the experimental procedure and the treatment of these data are the same for all systems. The total ionization cross sections used to obtain the individual cross sections were taken from the work of Sholette and Muschlitz.[11] The estimated error in these cross sections is $\pm$ 15 per cent.

CHAPTER V

RESULTS AND DISCUSSION

Various mechanisms can be proposed to explain the manner in which electronic excitation energy of an atom may be transferred to an atom or molecule. Two direct mechanisms are schematically represented in Figure 13. Consider now the upper and lower potential energy curves. During collision the internuclear distance between A^* and B diminishes until point X or Y is reached. In this region a spontaneous release of an electron can occur and the system passes by Franck-Condon transition to the lower potential curve. If this transition occurs at Y, then the molecular ion AB^+ may be formed (associative ionization). A transition occurring at X will result in the system passing to the lower curve at X' where the dissociation energy of AB^+ is exceeded. This will result in the formation of three particles: an electron, an ion, and a neutral.

A second direct mechanism is that of curve crossing. During collision the system (A^* + B) follows the upper potential curve as before, but there is a finite probability that at the internuclear separation r_c this system can cross over and follow the lower potential curve (A + B^*). The excess energy ΔE appears as kinetic energy of the products A and B^*. This will leave atom A in the ground state and molecule B^* in a pre-ionizing state such that subsequent ionization or dissociation may occur. Although this mechanism offers an

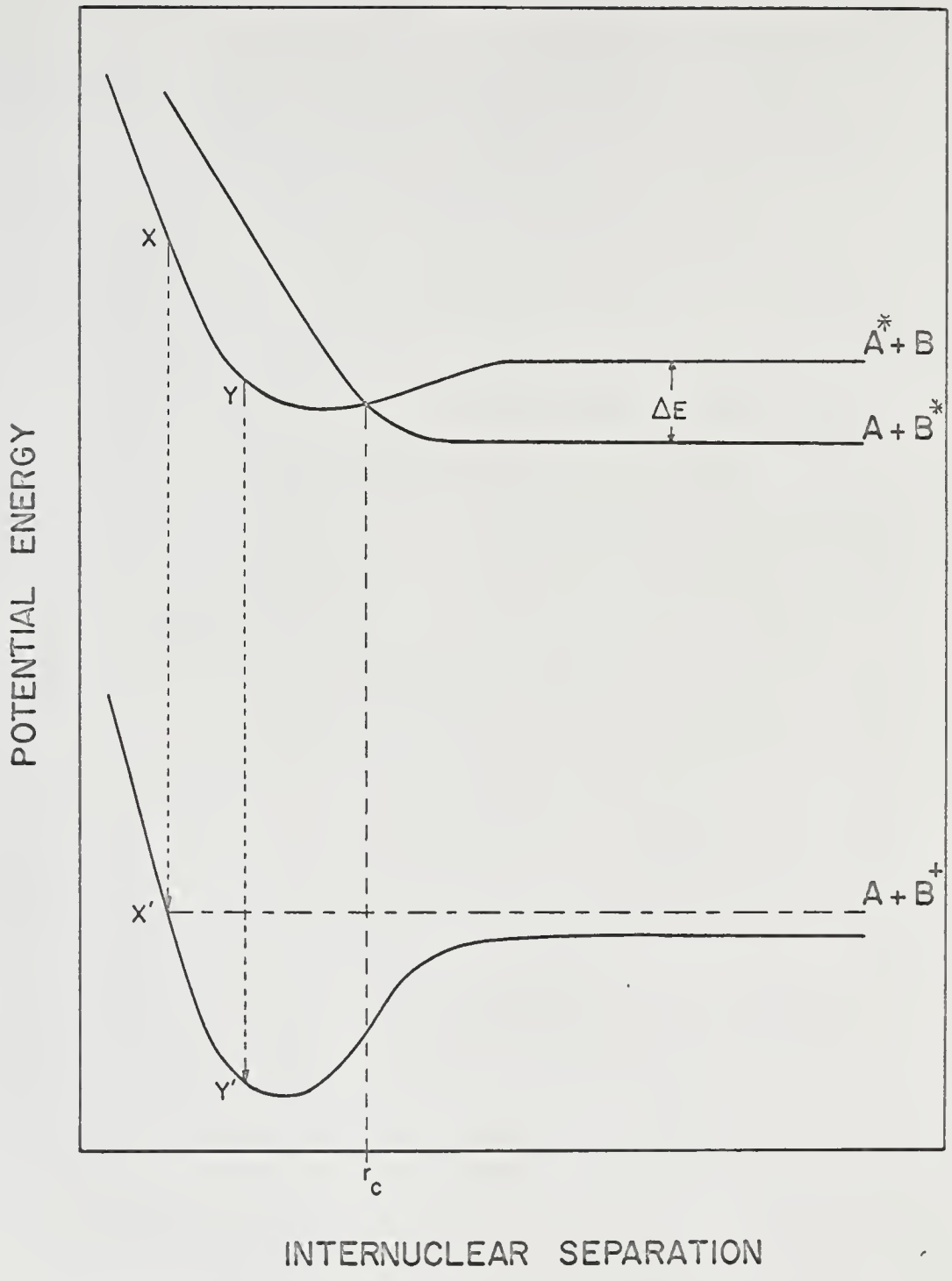

Figure 13. Schematic Diagram of Potential Energy Curves Describing Energy Transfer Processes.

adequate explanation for Penning ionization, it would be difficult to apply this explanation to systems in which associative ionization occurs.

Consider now another mechanism in which the excited A^* and B form a collision complex $(AB)^*$, which then can decay through various product channels. For this mechanism to be applicable, the lifetime of the complex must exceed the time for a few rotations of the complex. This mechanism has the distinct advantage over the previous one cited because it may be applied to all systems studied. Penton and co-workers[32] have employed a similar mechanism in explaining the isotope effect found in the He^* - H_2, He^* - D_2 systems. Because of its wide applicability, the collision complex mechanism will be used in analyzing the present results.

For simplicity, the results will be discussed in three sections: the rare gas systems, the He^* - O_2 system and the He^* - methane and methane - d_4 systems.

Rare Gas Systems

There is a significant change in the relative amounts of ionization of argon and krypton with changing metastable beam composition (Figures 8 and 9). The ion abundances and cross sections for each metastable state of helium are given in Table 2 with the results for the Ne^* - rare gas systems also.

In both metastable helium systems, the Penning ionization cross sections for the 2^1S_0 state are larger than those for the 2^3S_1

Table 2. Individual Ion Abudances and Ionization Cross Sections for the Rare Gas Systems.

System	Product Ion	Per Cent Ion Abundance $(2^1S_0)He^*$	Per Cent Ion Abundance $(2^3S_1)He^*$	Cross Section Å^2 $(2^1S_0)He^*$	Cross Section Å^2 $(2^3S_1)He^*$
He^* - Ar	Ar^+	91.5 ± 0.3	87.1 ± 0.2	7.0	6.6
	$HeAr^+$	8.5 ± 0.3	12.9 ± 0.2	0.6	1.0
He^* - Kr	Kr^+	92.6 ± 0.4	88.6 ± 0.2	8.3	8.0
	$HeKr^+$	7.4 ± 0.4	11.4 ± 0.2	0.7	1.0

System	Product Ion	Per Cent Ion Abundance (average)	Cross Section Å^2 (average)
Ne^* - Ar	Ar^+	81.6 ± 0.7	9
	$NeAr^+$	18.4 ± 0.7 (19.[illegible])	2
Ne^* - Kr	Kr^+	78.4 ± 0.5	-
	$NeKr^+$	21.6 ± 0.5 (23.[illegible])	-

state. The simple calculations of Ferguson[33] predicts a ratio of the singlet to triplet cross sections of about 1.1 to 1.2, which is due to the difference in van der Waals coefficients for the 2^1S_0 and 2^3S_1 states. The ratio of the cross sections determined in this study are 1.06 and 1.04 for the He^* - Ar and He^* - Kr systems, respectively.

The individual contributions for each of the metastable states of neon, $^3P_0$ and $^3P_2$, could not be determined for lack of sufficient data. Since the energy difference between these two states (16.62 and 16.71 eV) is small, a large difference in their behavior would not be expected. However, the relative population of these states does change according to the energy of the electrons used to produce them. Values for the ratio $^3P_2/^3P_0$ have been measured in the energy range 25 - 35 eV and vary from 0.51 to 1.39.[34] Within the experimental error of the measurements, the data shown for metastable neon systems are independent of electron energy and hence independent of the beam composition. Unresolved cross sections for both Penning and associative ionization have been calculated for the Ne^* - Ar system (Table 2), using the previously measured total ionization cross section of MacLennan.[18] The relative amount of associative ionization in the Ne^* systems is approximately twice as large as that occurring in the analogous reactions involving He^*.

Because of the existence of these associative ionization processes, it is tempting to envision these reactions as proceeding via a collision complex. Consider a mechanism whereby a collision complex is formed from an excited atom and an atom or molecule. This

complex may either eject an electron, forming the associative ion, or break up, leaving the excited helium atom in its ground state (1^1S_0) and the atom or molecule in a pre-ionizing state which may subsequently ionize. We will now restrict the discussion to an excited atom - atom system and look upon the mechanism for ionization in the following way:

$$(2^3S_1)He^* + Z \rightarrow (HeZ)^* \rightarrow HeZ^+ + e^-$$

$$\downarrow$$

$$He + Z^* \rightarrow Z^+ + e^-$$

In these experiments the target gas Z is in its ground state and has a singlet configuration. Conservation of spin demands that the pre-ionizing state have a triplet configuration. In order to form the atom in this pre-ionizing state Z^* without a reversal of electron spin, an electron exchange between the two atoms must occur to produce a helium atom in the singlet ground state; therefore, we would expect the probability for formation of Z^* from the singlet He^* (which does not require an electron exchange) to be greater than for the triplet. Considering the production of either ion as proceeding through the two competing reaction channels, the ratio (HeZ^+/Z^+) should be less for reactions involving the $(2^1S_0)He^*$ than for the $(2^3S_1)He^*$. The experimental results show that this ratio is smaller for 2^1S_0 metastable atoms. This effect is not observed in the metastable neon systems as would be expected from the above argument since both metastable states of neon have a triplet configuration.

$He^* - O_2$ System

As can be seen from Figure 10 and the values listed in Table 3, there is a definite difference (far outside the limits of experimental error) in the amount of O_2^+ and O^+ produced by each metastable state of helium. The data reported here agree within 20 per cent with previous results,[23] but is considered more precise since greater metastable beam intensity and increased detection sensitivity were obtained by modifications in the apparatus.

Adopting the same model as that for the rare gas systems, we may envision the ionization process proceeding in the following manner:

$$He^* + O_2 \rightarrow (HeO_2)^* \begin{cases} \rightarrow HeO^+ + (O + e^-) \\ \rightarrow HeO_2^+ + e^- \end{cases}$$

$$He + O_2^* \rightarrow O_2^+ + e^-$$

$$O^+ + (O + e^-)$$

The ions HeO_2^+ and HeO^+ were not observed in the mass spectra. Evidently the collision complex cannot be sufficiently stablized by the loss of an electron to produce these ions.

The production of O^+ ions is much more probable in collisions of singlet metastable atoms. The ratio of cross sections for the formation of this ion from the triplet versus singlet states is 0.42. A closer look into the various processes resulting in production of O^+ is in order.

Table 3. Individual Ion Abundances and Ionization Cross Sections for the Metastable Helium - Oxygen System.

System	Product Ion	Per Cent Ion Abundance $(2^1S_0)He^*$	Per Cent Ion Abundance $(2^3S_1)He^*$	Cross Section $Å^2$ $(2^1S_0)He^*$	Cross Section $Å^2$ $(2^3S_1)He^*$
$He^* - O_2$	O_2^+	85.4 ± 0.8	93.9 ± 0.3	12.0	13.1
	O^+	14.6 ± 0.8	6.1 ± 0.3	2.0	0.9

The pertinent electron impact appearance potentials are:[35]

$$e^- + O_2 \rightarrow O^+(^4S) + O^- \qquad (17.2 \pm 0.2)\text{eV} \qquad \text{V-1}$$

$$e^- + O_2 \quad O^+(^4S) + O(^1D) + e^- \qquad (19.2 \pm 0.2)\text{eV} \qquad \text{V-2}$$

$$e^- + O_2 \quad O^+(^2D) + O^- \qquad (20.4 \pm 0.2)\text{eV} \qquad \text{V-3}$$

If the O^+ production is considered to proceed through three possible reaction channels with the products shown above, then the third channel would be energetically impossible for 2^3S_1 helium. This offers a possible explanation for the observed decrease in the O^+ cross section, with decreasing fraction of singlet helium atoms in the beam.

He^* - CH_4 and He^* - CD_4 Systems

The experimental results for the ionization of methane and methane - d_4 on impact with thermal energy metastable helium atoms are shown in Table 4. Using the known appearance potential data for methane and methane - d_4,[36] it may be shown in each case that all ions are observed that correspond to energetically possible fragmentation processes.

There is but a slight difference in the amount and type of fragmentation occurring in the two systems for a particular metastable state, and these differences may well be within experimental error; however, the amount of fragmentation for the two metastable states is definitely different, and this difference should be considered real. It should be noted that only the CH_3^+, CD_3^+, CH_2^+ and CD_2^+ ion abundances are greater for $(2^1S_0)He^*$. No adequate explanation of these facts can be offered at the present time.

Table 4. Individual Ion Abundances for the Metastable Helium - Methane and Methane - d_4 Systems.

Product Ion	Per Cent Ion Abundance $(2^1S_0)He^*$	$(2^3S_1)He^*$	20 eV electrons[b]	21.3 eV photons[c]
CH_4^+	37.9 ± 1.3	46.7 ± 0.6	50.0	55.5
CD_4^+	34.4 ± 0.9	46.3 ± 0.4		
CH_3^+	56.7 ± 1.4	49.1 ± 0.6	41.0	35.4
CD_3^+	59.0 ± 0.9	51.0 ± 0.4		
CH_2^+	5.4 ± 1.4	4.2 ± 0.6	9.0	9.1
CD_2^+	6.6 ± 0.9	2.7 ± 0.4		

[b]See Ref. 23.

[c]See Ref. 37.

In Table 4 the mass spectra for impact of 20 eV electrons[23] and 21.3 eV photons[37] are also shown. There are a number of significant differences in comparison with the spectra corresponding to impact of metastable helium atoms. The most abundant ion is CH_3^+ for the He^* - CH_4 systems, but when the incident particles are electrons or photons, the parent ion CH_4^+ is the more abundant. Evidently, the interaction potential of the colliding species is a major factor in determing the fragmentation patterns.

Future Direction of Research

Future experiments with this apparatus should be extended to the study of the fragmentation patterns of other simple molecules: e.g., C_2H_6, C_2H_4, C_2H_2 and N_2O. Also, measurements of the negative ion spectra of $He^* + O_2$ would be invaluable in determining the reaction paths pertinent to the corresponding O^+ production.

Three mechanisms have been considered for reactions involving metastable atoms. Determinations of the velocity dependence of the cross sections could differentiate between a Franck-Condon mechanism and a curve crossing mechanism. Landau-Zener theory predicts a maximum in the velocity dependent cross section if curve crossing is involved. Measurements of the angular distribution of the product ions should be also undertaken to establish the kinematics of these reactions. Determination of the kinetic energy of Penning ions may yield useful information regarding the shape of the potential energy curves of these systems and the kinetic energy of the preionizing atoms which may be produced in such reactions.

The process, $X^{**} + M \rightarrow X^{+} + (M + e)$, has recently been observed to occur in collisions of highly excited rare gas atoms with various gases.[30] The cross sections for the processes are four orders of magnitude larger than Penning ionization cross sections. In the absence of the quenching field, such processes may occur and be investigated in the present apparatus. By studying the total amount and type of ionization with varying quenching field strength, these processes may be differentiated from Penning ionization. In the same manner, the field strength at which these highly excited states field ionize may be measured. The reaction, $Ar^{**} + He \rightarrow HeAr^{+} + e$, may also be studied. There is some evidence for the existence of states of Ar^{**} of energy as high as 18 eV.[26] If this pre-ionizing state is sufficiently long-lived and in the absence of a quenching field, $HeAr^{+}$ production is energetically possible for impact of excited argon atoms on helium.

APPENDICES

APPENDIX A

ORIGINAL DATA

Metastable Helium in Argon

Electron Energy (eV)	Per Cent Ion Abundance Ar^+	$HeAr^+$
26	88.1	11.9
30	88.6	11.4
40	89.2	10.8
50	89.4	10.6
60	89.5	10.5
80	90.3	9.7

Metastable Helium in Krypton

Electron Energy (eV)	Per Cent Ion Abundance Kr^+	$HeKr^+$
26	89.9	10.2
30	89.6	10.4
40	90.5	9.5
50	90.8	9.2
60	91.1	8.9
80	91.4	8.6

Metastable Neon in Argon

Electron Energy (eV)	Per Cent Ion Abundance Ar^+	$NeAr^+$
30	80.1	19.9
40	81.6	18.4
50	81.3	18.7
60	82.5	17.5
80	82.6	17.4

Metastable Neon in Krypton

Electron Energy (eV)	Per Cent Ion Abundance Kr^+	$NeKr^+$
30	77.4	22.6
40	77.9	22.1
50	78.3	21.7
60	78.9	21.1
80	79.7	20.3

Metastable Helium in Methane

Electron Energy (eV)	Per Cent Ion Abundance CH_4^+	CH_3^+	CH_2^+
26	44.8	50.2	5.0
30	42.6	52.4	5.0
40	42.6	52.7	4.7
50	41.5	53.5	5.0
80	40.0	53.8	6.2

Metastable Helium in Methane - d_4

Electron Energy (eV)	Per Cent Ion Abundance CD_4^+	CD_3^+	CD_2^+
26	43.3	53.0	3.7
30	42.7	53.4	3.9
40	41.1	54.8	4.1
50	39.6	55.6	4.8
60	38.6	55.8	5.6
80	38.8	56.1	5.1

Metastable Helium in Oxygen

Electron Energy (eV)	Per Cent Ion Abundance O_2^+	O^+
26	91.9	8.1
30	91.4	8.6
40	89.4	10.6
50	89.2	10.8
80	88.5	11.5

APPENDIX B

METASTABLE BEAM COMPOSITION

Table 5. Calculated Values of $R/(1 + R)$ as a Function of the Energy of Exciting Electrons.

Electron Energy (eV)	$R = 2^1S_0/2^3S_1$	$R/(1 + R) = 2^1S_0/(2^1S_0 + 2^3S_1)$
26	0.30	0.23
30	0.50	0.33
40	0.90	0.47
50	1.2	0.55
60	1.5	0.60
80	1.9	0.66

REFERENCES

1. N. F. Ramsey, Molecular Beams (Oxford University Press, London, 1956).

2. J. Ross, ed., Molecular Beams (Interscience Publishers, New York, 1966).

3. L. Dunoyer, Compt. Rend. 178, 1475 (1911).

4. O. Stern, Z. Physik 39, 751 (1926).

5. F. Knauer and O. Stern, Z. Physik 39, 764 (1926).

6. W. Gerlach and O. Stern, Ann. Physik 74, 673 (1924).

7. W. Gerlach and O. Stern, Ann. Physik 76, 163 (1925).

8. D. R. Herschbach, Molecular Beams (Interscience Publishers, New York, 1966), Chap. 9.

9. A. A. Kruithof and F. M. Penning, Physica 4, 430 (1937).

10. J. A. Hornbeck and J. P. Molnar, Phys. Rev. 84, 621 (1951).

11. W. P. Sholette and E. E. Muschlitz, Jr., J. Chem. Phys. 36, 3368 (1962).

12. V. Čermák and Z. Herman, Collection Czechoslov. Chem. Commun. 30, 169 (1964).

13. G. Breit and E. Teller, Astrophys. J. 91, 215 (1940).

14. H. K. Holt and R. Krotkov, Phys. Rev. 144, 82 (1966).

15. M. L. E. Oliphant, Proc. Roy. Soc. (London) A124, 228 (1929).

16. D. G. Greene, Proc. Roy. Soc. (London) 63, 876 (1950).

17. R. J. Stebbings, Proc. Roy. Soc. (London) A241, 270 (1957).

18. D. A. MacLennan, Phys. Rev. 148, 218 (1966).

19. V. Čermák, J. Chem. Phys. 44, 3374 (1966).

20. J. L. G. Dugan, H. L. Richards and E. E. Muschlitz, Jr., J. Chem. Phys. 46, 346 (1967).

21. W. P. Jesse and J. Sadauskis, Phys. Rev. 100, 1755 (1955).

22. Z. Herman and V. Čermák, Collection Czechoslov. Chem. Commun. 31, 649 (1966).

23. E. E. Muschlitz, Jr. and M. J. Weiss, Atomic Collision Processes (North-Holland Publishing Company, Amsterdam, 1964), p. 1073.

24. W. Kaul, P. Seyfried and R. Taubert, Z. Naturforsch. 18a, 432 (1963).

25. W. Kaul, Compt. Rend. Conf. Intern. Phenomnes Ionisation Gas 6^{e}, Paris 1, 169 (1963).

26. M. S. B. Munson, J. L. Franklin and F. H. Field, J. Phys. Chem. 67, 1542 (1963).

27. E. E. Muschlitz, Jr., H. D. Randolph and J. N. Ratti, Rev. Sci. Instr. 33, 446 (1962).

28. G. M. Smith and E. E. Muschlitz, Jr., J. Chem. Phys. 33, 1819 (1960).

29. V. Čermák and Z. Herman, Collection Czechoslov. Chem. Commun. 29, 953 (1964).

30. H. Hotop and A. Niehaus, J. Chem. Phys. 47, 2506 (1967).

31. H. Margenau and G. M. Murphy, The Mathematics of Physics and Chemistry (D. Van Nostrand Company, Inc., New York, 1956), p. 517.

32. J. R. Penton, S. Kardonsky and E. E. Muschlitz, Jr., Abstracts of Papers Published at 13th Mass Spectrometry Conference, A.S.T.M. Committee E-14, May, 1965, p. 230.

33. E. E. Ferguson, Phys. Rev. 128, 210 (1962).

34. R. J. Hammond, unpublished data.

35. H. D. Hagstrum, J. Chem. Phys. 23, 1178 (1955).

36. F. H. Field and J. L. Franklin, Electron Impact Phenomena (Academic Press, New York, 1957).

37. B. Brehm and E. von Puttkamer, Z. Naturforsch. 22a, 8 (1967).

BIOGRAPHICAL SKETCH

John Austin Herce was born in Newark, New Jersey, on November 10, 1940. After graduating from Valley High School in Orange, New Jersey, he entered Villanova University, Villanova, Pennsylvania. He received the Bachelor of Science Degree with major in Chemistry in June, 1962 and the Bachelor of Science Degree with major in Physics in June of the following year.

In September, 1963, he entered the Graduate School of the University of Florida. During that time he held the positions of graduate assistant and Petroleum Research Fellow in the Department of Chemistry.

This dissertation was prepared under the direction of the chairman of the candidate's supervisory committee and has been approved by all members of that committee. It was submitted to the Dean of the College of Arts and Sciences and to the Graduate Council, and was approved as partial fulfillment of the requirements for the degree of Doctor of Philosophy.

December, 1967

E. Ruffin Jones

Dean, College of Arts and Sciences

Dean, Graduate School

Supervisory Committee:

E E Muschett, Jr.

Chairman

S O Colgate

J D Windham

L L Bailey